Renewable and Sustainable Energy Reviews 26 (2013) 20–33

Contents lists available at ScienceDirect

Renewable and Sustainable Energy Reviews

journal homepage: www.elsevier.com/locate/rser

Energy balance of internal combustion engines using alternative fuels

M.J. Abedin *, H.H. Masjuki, M.A. Kalam, A. Sanjid, S.M. Ashrafur Rahman, B.M. Masum

Centre for Energy Sciences, Faculty of Engineering, University of Malaya, 50603 Kuala Lumpur, Malaysia

ARTICLE INFO

Article history:
Received 20 February 2013
Received in revised form
8 May 2013
Accepted 20 May 2013
Available online 14 June 2013

Keywords:
Energy balance
Thermal balance
Heat loss
Heat transfer correlations
Alternative fuels

ABSTRACT

This paper reviews the literature available concerning the energy balance of internal combustion engines operating on alternative fuels. Global warming and energy crisis are among the most important issues that threaten the peaceful existence of the man-kind. More usage of alternative fuels and energy loss minimization from automotive engines can be an effective solution to this issue. The energy balance analysis gives useful information on the distribution of supplied fuel energy in the engine systems and identifies the avoidable losses of the real engine process with respect to ideal process. It is a very widely used tool, mostly used for the layout of the engine components. The basic energy balance theory has been discussed in details along with the variations in energy balance approaches and terms. The wall energy loss may vary to a great extent depending on the selection of heat transfer correlations. The theoretical energy balance also explored in this paper with help of thermodynamic models. There are some significant variations observed in energy balance when the engine operating fuel is changed and devices like turbocharger, supercharger etc. are used to boost the intake air pressure. The review extends to the energy balance study of low heat rejection engines (LHR) as well as the effects of engine variables and design factors on energy balance.

Contents

1. Introduction . . . 21
2. Theory of energy balance . . . 23
   2.1. First approach to energy balance . . . 23
   2.2. Second approach to energy balance . . . 23
   2.3. Heat transfer correlations for wall heat loss calculation . . . 24
3. Energy balance using alternative fuels . . . 25
   3.1. Energy balance using alcohols . . . 25
   3.2. Energy balance using biodiesels . . . 25
   3.3. Energy balance using hydrogen fuel . . . 26
   3.4. Energy balance using LPG . . . 27
4. Energy balance of LHR engines . . . 27
5. Theoretical investigation of energy balance . . . 28
   5.1. Multi-zone thermodynamic models . . . 28
   5.2. Energy balance using multi-zone models . . . 28
   5.3. Single-zone thermodynamic models . . . 28
   5.4. Outcome of the single-zone models . . . 29
6. The effects of the engine operating parameters and design factors on energy balance . . . 29
7. The roles of turbocharger and supercharger on energy balance . . . 30

Abbreviations: BSFC, brake specific fuel consumption [g/kW h]; BTDC, before top dead center; CNG, compressed natural gas; CR, compression ratio; DI, direct injection; EVO, exhaust valve opening; EHN, ethylexyl nitrate; EGR, exhaust gas recirculation; IVC, inlet valve closing; JME, jatropha methyl ester; LHV, lower heating value [KJ/Kg]; LPG, liquid petroleum gas; LHR, low heat rejection; MBT, maximum brake torque; POME, palm oil methyl ester; PFI, port fuel injection; SME, soybean oil methyl ester; TDC, top dead centre; WOT, wide-open throttle; YGME, yellow grease methyl ester.

* Correspondence to: Department of Mechanical Engineering, University of Malaya, 50603, Kuala Lumpur, Malaysia. Tel.: +60 149 901 927; fax: +60 379 675 317.
E-mail addresses: joynul06me@yahoo.com, joynul06me@siswa.um.edu.my (M.J. Abedin).

1364-0321/$ - see front matter © 2013 Elsevier Ltd. All rights reserved.
http://dx.doi.org/10.1016/j.rser.2013.05.049

8. Conclusions . . . 31
Acknowledgments . . . 31
References . . . 32

1. Introduction

The fast depletion of fossil fuels, the alarming rate at which the Earth's atmosphere is getting polluted, the increased impact of global warming on Earth and the stringent anti-pollution laws imposed in certain countries have created a stimulus to explore and evaluate alternative fuels for internal combustion engines. As the cost of liquid hydrocarbons is increasing day by day, the interest in alternative fuels for automotive engines is more stimulated in recent years [1–3]. The use of alternative fuels like alcohols, biodiesels, hydrogen etc. in automotive engines is weighty in this context. However, the principal job is, the selected alternative fuel has to serve its purpose best.

An internal combustion (IC) engine is a complex of machinery, instrumentation and services, all of which must work together as a whole. IC engines can be considered as a thermodynamic 'open system', which is a powerful concept to understand the thermodynamic behaviour of a system. It is linked to the idea of 'control volume', a space enclosing the system and surrounded by an imaginary surface often known as 'control surface' (Fig. 1). The advantage of this concept is that once one has identified all the mass and energy flows into and out of a system, it is easy to visualize the inside picture of that system by drawing up an energy balance sheet of inflows and outflows [4]. This energy balance is useful at early stage of designing an IC engine and its subsystems such as cooling system, lubricating oil system, ventilation etc. The researchers have applied different methodology for IC engine energy balance. In this literature the authors will discuss two different methodologies that have found helpful as a means of pulling all the disparate elements together, and which is applied, explicitly or implicitly, throughout the paper. At present, the alternative fuels like alcohols, biodiesels, hydrogen etc. are being used frequently in IC engines. So, the energy balance study of IC engines using these fuels and also the investigation of the effects of different engine variables and design factors will accelerate the feasibility of alternative fuel usage in IC engines. The researchers have used various heat transfer correlations to calculate coolant heat loss or wall heat loss in those experiments; but it requires investigation to find out which one suits best for a particular engine. Moreover, the energy balance of a turbocharged or supercharged engine needs a separate calculation to consider the energy flows from in and out of the turbine, compressor and cooler. Besides, in-cylinder heat transfer characteristics of those engines are greatly effected in the sense that both devices consume fuel heat/exhaust energy which is utilized to achieve improvements in combustion process by increasing the charge quality (i.e. increasing the intake air density) to facilitate complete combustion. These are strong drivers for research, development and demonstration of new technology and alternative fuel for IC engines. The above information were very much scattered and needed to collect under one literature to understand the basic first law analysis (energy balance) of IC engines. Considering the depth of this topic, the multitude of recent studies as well as on-going efforts on this theme, its magnitude on future automotive industry and its intrinsic intricacy, the authors have tried to offer a comprehensive and extensive review article for the first time on this topic. Therefore, the review is aiming to provide the following contents and information.

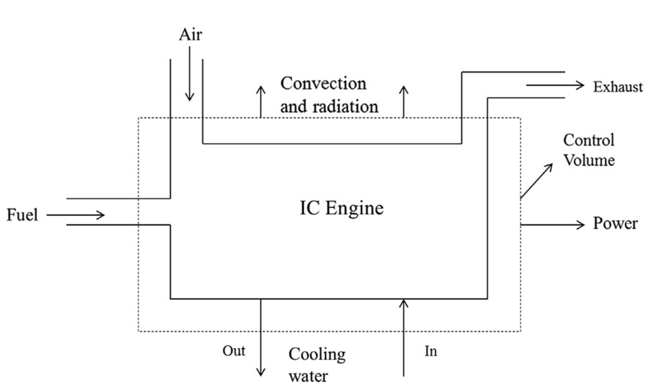


Fig. 1. Control volume of IC engine showing energy flows (re-drawn from [4]).

Two different approaches will be discussed to perform energy balance in IC engines in Section 2. In second approach, a suitable heat transfer correlation is required to compute the wall heat losses. So the details of some heat transfer correlations along with their mathematical models and engine performances for both diesel and gasoline engines will be talked over in Section 2.3. The energy balance using alternative fuels will be investigated in Section 3 considering the effects of thermo-chemical properties of those fuels and also the effects of engine variables on energy balance. A separate section (Section 4) will be allotted to the Low heat rejection (LHR) engine energy balance because in this type of engines, the coolant heat losses are intentionally reduced to a great extent by applying ceramic materials on cylinder walls, head, piston top etc. Theoretical investigations of energy balance and heat transfer modelling are effective tools for overall engine performance prediction, sensitivity analysis of various engine operating parameters, new technology developments and evaluation. These will be explored in Section 5. The effects of engine design factors and operating parameters on energy balance will be investigated in Section 6 and is followed by another section (Section 7) which introduces the turbocharging and supercharging effects on energy balance. Finally, the conclusion section summarizes the gaps remaining in this field and the core findings of this effort. The rest of the introduction and the whole paper follow this sequence.

The energy balance of IC engines yields the allocation of the supplied fuel energy to the various engine components. This type of analysis permits the designer to evaluate the internal energy variation as a function of the energy transfers across the boundaries as heat or work and the enthalpies associated with the mass flow crossing these boundaries [5]. The energy balance of IC engines is basically an analysis of the first law of thermodynamics which is also called as the energy balance or the heat balance or thermal balance. On the other, the second law analysis which is also known as the availability or exergy balance is more complicated and leads to the irreversibility identification [6,7]. The most of the studies concerning second law application to IC engines are based on a preceding first law mathematical modelling of the various in-cylinder processes and its subsystems. The thermodynamic details of a thermal system operation can be better understood by performing energy balance of the system.

The researchers have done the energy balance of the IC engines in different terms and ways but the foundation is the first law of

Nomenclature

A	heat transfer area [m^2]
B	bore diameter [m]
C_p	specific heat at constant pressure [kJ/kg K]
C_v	specific heat at constant volume [kJ/kg K]
C	specific heat [kJ/kg K]
h_g	heat transfer coefficient for gasses in the cylinder [W/m^2 K]
K_g	thermal conductivity of the cylinder gas [W/m K]
L	connecting rod length [m]
$\dot{m}$	mass flow rate [kg/s]
P	pressure [kPa]
Q	heat [kJ]
R_g	gas constant [kJ/kg K]
R	crank radius [m]
S	stroke [m]
T	temperature [K]
U	internal energy [J]
V	volume [m^3]
V_{mp}	mean piston speed [m/s]
X	distance from top dead center [m]

Greek symbols

γ	specific heat ratio
λ	air–fuel equivalence ratio
Ø	fuel-air equivalence ratio φ crank angle [degree]
φ_s	start of combustion or heat addition [degree]
$\Delta\varphi$	combustion duration [degree]
ω	average cylinder gas velocity [m/s]

Dimensionless numbers

Re	Reynolds number
Nu	Nusselt number
Pr	Prandtl number

Subscripts

a	air
b	brake
c	clearance
cl	calorimeter
cv	control volume
d	displacement
exh	exhaust
f	fuel
g	gas
gx	gas exchange
ic	incomplete combustion
w	water
wh	wall loss
l	wall
mp	mean piston
un	unaccounted
rc	real combustion
rg–bb	real gas and blow-by
s	supplied

thermodynamics [8–13]. The major energy balance terms are the brake power, the cooling loss or cooling heat loss and the exhaust loss or exhaust heat loss. The undetermined energy losses are termed as the unaccounted heat loss or the miscellaneous heat loss. It covers mainly the convection and radiation heat losses. Though, some researchers [5,9,11,12] considered the lubricating oil loss (if separately cooled) as miscellaneous heat loss. So there will be some fluctuations in the numerical values of unaccounted heat loss. The exhaust heat loss can be calculated either by assuming the specific heat of air, at mean exhaust temperature, as the average specific heat of the gases or by using exhaust calorimeter [4]. A substantial part of the exhaust loss (12%) is radiated to the surroundings and the remainder ends up in the cooling medium. A considerable amount of the friction power (around 50%) is dissipated between the piston and piston rings and cylinder walls and is lost as heat to the cooling medium. The rest of the friction power is dissipated in the bearings, valve mechanism or drives, auxiliary devices and is lost as heat to the lubricating oil or surroundings. Thus the coolant heat loss consists of heat transferred to the exhaust valve and port in the exhaust process, and a substantial fraction of the friction work [5].

Another approach [14,15] of energy balance is the consideration of the following terms: incomplete combustion loss, real combustion loss, wall heat loss, gas exchange loss, real gas and blow-by loss and mechanical loss. Here the mechanical loss and the wall heat loss are considered as the cooling loss. The exhaust loss is sub-divided into several terms because exhaust gas enthalpy has following components [5]: sensible enthalpy (60%), incomplete combustion loss (20%), exhaust kinetic energy (7%) and heat transfer to the exhaust (12%). The most important thing for wall heat loss calculation is the selection of an appropriate heat transfer correlation. The available engine instantaneous heat transfer coefficients are classified as time-averaged coefficients, instantaneous spatially averaged coefficients and instantaneous local coefficients. The instantaneous local heat transfer coefficients are not uniform over the combustion chamber and may be required for thermal stress calculations. The overall time-average heat transfer coefficient may be adequate for some design purposes. The instantaneous spatially averaged heat transfer coefficients, [16–18] etc., are useful for engine performance analysis [5]. The details of these correlations will be discussed in the theory section.

The theoretical energy balance of IC engines is performed by some researchers [11,19,20] using some thermodynamic models. The thermodynamic models are based on the first law of thermodynamics. These models are a complete package for engine heat transfer analysis. They are very effective energy balance tools for the measurement of engine performance and other engine operating parameters. Temperature, pressure and heat fluxes are estimated with respect to crank angle or time. The heat loss from the combustion chamber to the cylinder walls are taken into account using some empirical and semi-empirical correlations. These models are classified into two groups namely single-zone models and multi-zone models [21]. If we consider compression ignition (CI) engines, these models extent from ideal cycle simulation to overall engine simulation and to the more frequently applied phenomenological filling and emptying models. In spark ignition (SI) engines, dissociation is considered because combustion is near to stoichiometric condition [6]. The single-zone models are simple and have reasonable accuracy. They treat the working fluid inside the engine as a uniform mixture. If these models do not consider any flow field dimensions then they are

called as zero dimensional models [6]. The more accurate, developed and complicated models which also cover engine emissions are two zone [22–24], four zone or multi zone models [11,20,25,26]. They are based on the numerical calculation of mass, momentum and energy conservation equations in either one, two or three dimensions to follow the propagation of flame or combustion front within the engine combustion chamber.

The brake power of automotive engines is usually in the range 25% to 28% for SI engine and 34% to 38% for CI engine when operated on conventional fuels. The energy balance using conventional fuels shows: 17–26% cooling loss, 36–50% exhaust loss and 3–10% other losses for SI engines and 16–35% cooling loss, 23–37% exhaust loss and 2–6% other losses for CI engines [5,27]. But when the conventional fuel is replaced or blended [12,21,28,29] and/or fumigated [8,11,19] with alternative fuels, the heat losses and the engine performance are varied to a considerable extent. The variations are due to the following reasons: Alcohols exhibit cooling effect and have higher octane rating compared to fossil fuels; biodiesels have excessive oxygen molecules which lower its calorific value, oxygen-rich biodiesels promote better combustion; hydrogen fuel has higher specific heat ratio, higher octane number, lower flammability limits and higher heating value than gasoline. The energy balance of LHR engines is not similar with standard IC engines, because the ceramic coatings of low thermal conductivity reduce the cooling heat loss to a great extent. So it has been discussed in a separate section. The fuel consumption rate and the heat losses from engines are related; by reducing the amount of heat lost to the surroundings, fuel consumption rate can be improved.

The following engine variables and design factors affect the energy balance of IC engines: engine speed, load, equivalence ratio, compression ratio (CR), spark timing, spark plug location, valve diameter, valve lift, flame speed, swirl, squish, cylinder head material. The effects of these variables may vary from engine to engine and fuel to fuel.

2. Theory of energy balance

In this section, two different approaches of energy balance will be explored. According to first approach, we only need the coolant inlet and outlet thermocouple readings for coolant heat loss calculation and exhaust gas thermocouple readings for exhaust heat loss calculation. In the second approach, coolant and exhaust losses will be sub-divided into several heat loss terms and some theoretical models will be applied to predict and calculate heat losses. There are many heat transfer correlations which are not suitable for all kinds of engine because they are developed based on different engine experiments and assumptions. For energy balance calculation by the second approach, heat transfer correlations are required for the calculation of wall heat loss or coolant heat loss. The last part of this section gives a detail idea of heat transfer correlations available in the literature showing their physical structure, variables, assumptions and comparative engine performances.

2.1. First approach to energy balance

If we consider the IC engine as a control volume (surrounded by control surface), than the energy flows from and to the engine will be as follows [4]:

In: fuel, with its associated heat of combustion plus air, consumed by the engine.

Out: brake power, exhaust loss, cooling medium loss and convection and radiation to the surroundings.

The steady flow first law equation [4,5] for this control volume will be

$$Q_s = P_b + Q_w + Q_{exh} + Q_{misc} \tag{1}$$

The terms of Eq. (1) are explained below

The energy supplied by the fuel (Q_s) is

$$Q_s = \dot{m}_f \times Q_{LHV} \tag{2}$$

where $m_{\cdot f}$ is the mass flow rate of fuel and Q_{LHV} is the calorific value of fuel.

The output power delivered by the engine or the engine brake horse power (P_b), is given by the equation

$$P_b = 2 \times \pi \times N(rev/s) \times T(N.m) \times 10^{-3} \tag{3}$$

The amount of heat, which is carried away by the cooling water (Q_w), is given by

$$Q_w = \dot{m}_w \times C_w \times \Delta T_w \tag{4}$$

If we know the necessary heat to increase the temperature of the total mass (air+fuel) with respect to outside ambient air temperature (T_a) to the temperature of the exhaust gas (T_g), then we can measure the amount of heat lost with the exhaust gases. The specific heat of air at mean exhaust temperature is considered as the average specific heat (C_g) of the gases for this case [12].

$$Q_{exh} = (\dot{m}_f + \dot{m}_a) \times C_g \times (T_g - T_a) \tag{5a}$$

Another approach for exhaust loss calculation is the use of exhaust calorimeter [4,9]. This is an air to water heat exchanger where the gas is cooled to a moderate temperature (not below 60 °C, because it's the dew point for the exhaust gas) and heat loss is calculated by observing the cool water flow and temperature rise. The formula will be

$$Q_{exh} = \dot{m}_w \times C_w \times \Delta T_w + (\dot{m}_f + \dot{m}_a) \times C_p \times T_{cl} \tag{5b}$$

The amount of heat carried away by the lubricating oil (Q_{oil}) can be computed by using this equation

$$Q_{\text{oil}} = \dot{m}_{\text{oil}} \times C_{\text{oil}} \times \Delta T_{\text{oil}} \tag{6}$$

The unaccounted heat loss (Q_{un}) can be found by applying subtraction rule [8–10]

$$Q_{un} = Q_s - (P_b + Q_w + Q_{exh} + Q_{oil}) \tag{7}$$

2.2. Second approach to energy balance

Another approach has been conducted for the energy balance of IC engines, in terms of incomplete combustion loss (Q_{ic}), real combustion loss (Q_{rc}), wall heat loss (Q_{wh}or $dQ_l/d\varphi$), gas exchange loss (W_{gx}), real gas and blow-by loss (Q_{rg-bb}) and mechanical loss (will be found by subtraction) [14,15].

The fuel conversion efficiency for constant volume process is given by

$$\eta_{cv} = 1 - CR^{1-\gamma} \tag{8}$$

where CR is compression ratio and γ is the ratio of specific heats at constant volume and pressure.

The maximum possible indicated work is equal to

$$Q_s \times \eta_{cv} \tag{9}$$

The indicated work is given by the integration of $P.dV$ over the entire engine cycle, $\eta_i = \oint P.dV$

In ideal cases, $\eta_{cv} = \eta_i$ but in reality, $\eta_{cv} \rangle \eta_i$ due to the engine losses. The incomplete combustion loss (Q_{ic}) can be computed by

measuring the concentration of unburned HC, H_2 and CO at the exhaust gas.

The real combustion loss (Q_{rc}) can be found by integration [14,15]

$$\eta_{rc} = \frac{1}{dQ_s}\int \frac{dQ_s}{d\varphi}.r_{cv,\varphi}.d\varphi \tag{10}$$

where $dQ_s/d\varphi$ is heat release rate and $r_{cv,\varphi}$ is a constant volume ratio. $r_{cv,\varphi} = (1-(1/CR_\varphi^{\gamma-1})/1-(1/CR^{\gamma-1})$ and $CR_\varphi = V_c + V_d/V_\varphi$ where V_c, V_φ and V_d are the cylinder clearance volume, the cylinder volume at a crank angle, φ and the cylinder displacement volume, respectively.

The wall heat loss is expressed as [5]

$$\frac{dQ_l}{d\varphi} = h_g \times A \times (T_g - T_l) \tag{11}$$

The wall temperature should not exceed 180–200 °C to assure thermal stability of the lubricating oil and structural strength of the wall [27]. Some mathematical models will be given in Section 2.3 for the calculation of hg

The gas exchange loss (W_{gx}) can be calculated by computing the mean indicated pressure at the time of gas exchange.

$$P_{mi,gx} = \frac{1}{V_d}\int_{EVO}^{IVC} P\, dV \tag{12}$$

The summation of the above losses with the addition of $Q_s \times \eta_{cv}$ is slightly lower than the indicated work and expressed as

$$Q_s - (Q_s.\eta_{cv} + Q_{ic} + Q_{rc} + Q_{wh} + W_{gx}) > P_{mi,gx}V_d = \oint P\, dV \tag{13}$$

The real gas and blow-by losses (Q_{rg-bb}) will be [14,15]:

$$Q_{rg-bb} = Q_s - (Q_s\,\eta_{cv} + Q_{ic} + Q_{rc} + Q_{wh} + W_{gx}) - P_{mi,gx}\,V_d \tag{14}$$

2.3. Heat transfer correlations for wall heat loss calculation

For wall heat loss (Q_{wh}) or $dQ_l/d\varphi$ calculation, there are several empirical and semi-empirical correlations available. Depending on the variables, they are divided into two groups [30]. The first group's correlations are based on the equation, $h(t) = f[V_p, P_g(t), T_g(t)]$ and the second group's correlations are based on the equation, $Nu(t) = f[Re(t), \text{gas} \times \text{properties}]$

The first group is represented by Eichelberg, Nusselt and Pflaum correlations and the second group is represented by Sitkei, Annand and Woschni correlations. The variables of all correlations have been presented in the nomenclature table.

Eichelberg's correlation [31]:

$$h_g = 7.67 \times 10^{-3}(V_{mp})^{1/3}(P \times T_g)^{1/2} \tag{15}$$

This correlation (Eq. (15)) is the modified version of the first heat transfer model (based on natural convection), developed by Nusselt in 1923. This model can describe the effects the engine parameters on the heat loss for the very first time. The correlations after this are based on forced convection. This model has been widely used to investigate heat transfer in two-stroke and four-stroke engines [30].

Sitkei's correlation [32]:

$$h_g = 2.36 \times 10^{-4}(1+b)\frac{(P \times V_{mp})^{0.7}A^{0.3}}{T^{0.2}(4V)^{0.3}} \tag{16}$$

where $b = 0-0.35$, depends on the combustion chamber design. This model (Eq. (16)) was developed based on the diesel engine experiments.

Annand's correlation [16]:

$$h_g = a \times \frac{K_g}{B}Re^{0.7} + b\frac{(T_g^4 - T_l^4)}{(T_g - T_l)} \tag{17}$$

where $a = 0.35-0.8$ and $b = 4.3 \times 10^{-9}$ W/m^2 K^{-4} for SI engines. This is the only model (Eq. (17)), which is developed for the both CI and SI engines and also considers the radiation heat transfer. The constant b differs depending on the type of engine.

Woschni's correlation [17]:

$$h_g = C_0\left[B^{-0.2} \times P^{0.8}\left((C_1 \times V_{mp}) + C_2 \times \frac{V_d \times T_1}{P_1 \times V_1}(P_\theta - P_m)\right)^{0.8} \times T^{-0.53}\right] \tag{18}$$

where P_1, V_1 and T_1 are reference state properties i.e. IVC; P_m is the motored cylinder pressure at the same crank angle as P; the constants $C_0 = 110-130$, C_1 [–] and C_2 [m/s K] are given in Table 1.

All models except Woschni, assumes that the mean piston speed is proportional to the average gas velocity. Woschni first introduced the time dependent gas velocity for better computation of the heat transfer coefficient. According to Hohenberg, Woschni's model under-estimates and over-estimates the heat transfer coefficient during compression and combustion stroke, respectively [5,30]. So he introduced a new correlation.

Hohenberg's correlation [18]:

$$h_g = C_1 \times V^{-0.06} \times P^{0.8} \times T^{-0.4}(C_2 + V_{mp})^{0.8} \tag{19}$$

where P is the instantaneous pressure [bar]; the constants $C_1 = 130$ and $C_2 = 1.4$. This model (Eq. (19)) was developed based on the six different types of engines.

In a single cylinder, four strokes, air cooled and CNG fuelled SI engine, the models have performed as follows [30].

Hohenberg stated that Woschni's correlation over estimates average heat flux during a cycle. Moreover, he mentioned about its difficulty of use which led him to develop his own correlation. Woschni's correlation is difficult to use because it needs motoring pressure data and more calculation time compared to others. On the other hand, Hohenberg's correlation is the improvement of Woschni's correlation which mitigates all drawbacks of Woschni's correlation. Moreover, it has been reported that the deficiency of Eichelberg correlation during compression stroke is removed through this correlation. These things have made Hohenberg correlation more acceptable than others for SI engine [30,33,34]. Like Hohenberg correlation, Eichelberg correlation is easy to use; requires less calculation time and almost no tuning has to be performed. Annand correlation is different from others in the sense that it includes radiation term. Lounici et al. [30] have stated that tuning coefficient has a big influence on its engine performance. When the constant (a) in Annand's correlation was set at 0.8, the heat transfer coefficient was overestimated; hence the

Table 1
Constants for Woschni's correlation.

Stroke	C_1	C_2
Intake and Exhaust	6.18	0
Compression	2.28	0
Combustion and Expansion	2.28	3.24×10^{-3}

Table 2
Comparison of heat transfer correlations.

Correlations	Difficulty in use	Calculation time	Accuracy	Tuning
Hohenberg	Not difficult	Lower	Good	Not required
Eichelberg	Not difficult	Lower	Acceptable	Not required
Woschni	Difficult	Higher	Acceptable	Required
Annand	Not difficult	Lower	Depends on tuning	Big influence
Sitkei	Not difficult	Lower	Not acceptable	Required

cycle performance was underestimated. This made Annand's correlation less interesting for SI engine. Again, like Annand's correlation, Sitkei correlation underestimates heat transfer coefficient and its accuracy for SI engine is not that good [30]. Table 2 can be a good guidance for researchers to choose a suitable heat transfer correlation for SI engines.

3. Energy balance using alternative fuels

3.1. Energy balance using alcohols

Ajav et al. [8] investigated the energy balance of a single cylinder diesel engine operating on diesel, ethanol-diesel blends and fumigated ethanol–diesel fuel. The balance was done in terms of output work, cooling water heat loss, exhaust heat loss, lubricating oil heat loss and other unaccounted losses. The percentage of useful work or output work with respect to the supplied fuel energy for diesel engine was 28.68%, whereas it was 28.73, 31.06, 31.95 and 32.89% for 5, 10, 15 and 20% ethanol–diesel blends, respectively. On the other hand, for fumigated ethanol, useful work was 28.52% for cold fumigation and 28.14% for preheated fumigation. So with the increase of ethanol percentage in ethanol–diesel blends, the amount of useful work increased compared to diesel fuel. This happened due to the cooling effect and higher combustion efficiency of ethanol as compared to diesel fuel. As a consequence, the cooling water, exhaust and lubricating oil heat losses decreased with the increase of ethanol blending compared to conventional diesel fuel. They also observed the effects of load variations on engine energy balance. With the increase of engine loads, the amount of useful work increased while other losses decreased. The stiffness of the curves decreased at the higher engine loads. Though, the energy balance of the engine was not significantly different for fumigated ethanol, 5% and 10% ethanol–diesel blends, but there were notable differences for 15% and 20% ethanol–diesel blends at a 5% level of significance, compared to conventional diesel fuel. A reduction in the compression ratio (12 to 8) reduced the brake power by 4% and increased the exhaust loss by 5% when ethanol fuel used [6]. Alasfour [28] experimentally investigated the energy balance of a single cylinder SI engine using butanol (30%vol) with gasoline fuel. He found that the heat loss to the cooling water remains constant because of constant water flow rate. The exhaust heat loss was higher for gasoline fuel compared to butanol–diesel blend during the lean operation due to the higher exhaust gas temperature. But after reaching the maximum exhaust gas temperature (at fuel–air equivalence ratio of $Ø \approx 1.0$), the exhaust heat loss started to decrease for gasoline fuel, because of the reduced air density. The unaccounted loss was also higher for gasoline fuel than the butanol–gasoline blend at the region, $Ø = 0.8–1.0$ due to the higher engine cycle temperature. But during the rich operation ($Ø > 1.0$), the unburned butanol–gasoline mass increased which led to same exhaust heat loss at the region $Ø \approx 1.2$, for both fuels. Ethanol has higher octane rating, but butanol features a lower heating value (LHV) much closer to gasoline and far less corrosive. The octane rating of butanol can be improved by producing isomer (*iso*-butanol) of *n*-butanol [35]. A comparative study among methanol, ethanol, gasoline, methane, propane, hexane and hydrogen shows methanol and ethanol give higher brake power than other fuels at the engine condition; brake mean effective pressure (BMEP)= 325 kPa, $Ø = 1$ and maximum brake torque (MBT) timing. Methanol and ethanol fuel exhibit less exhaust loss than other fuels except methane [36]. Abu-Zaid et al. [37] reported that 15% (vol.) methanol plus 85% (vol.) gasoline blend requires lower brake specific fuel consumption (BSFC) and exhibits lower heat loss.

3.2. Energy balance using biodiesels

Ramadhas et al. [21] investigated theoretically and experimentally, the energy balance of a diesel engine operating on rubber seed oil methyl ester, diesel fuel and their blends. They used Runge–Kutta 4th order method (RK-4) to solve first law equation and Hohenberg's correlation [18] for wall heat loss calculation. The brake power, hence the brake thermal efficiency of biodiesel was lower than the diesel fuel due to the presence of oxygen molecule. Excessive oxygen molecule lowers the calorific value of the biodiesel. The peak temperature was higher and the peak pressure was lower while using rubber seed oil. So, the heat losses from the biodiesel fuelled engine were higher than the diesel fuelled engine. The brake power, the peak temperature and pressure increased with the increase of CR for all fuels and the results were opposite for relative air-fuel ratio. Canakci and Hosoz [38] determined the energy balance of diesel engine operating on soybean oil methyl ester (SME), yellow grease methyl ester (YGME), No. 2 diesel fuel and their 20% blends. The BSFC of SME and YGME was 12.2% and 12.9% higher than No. 2 diesel fuel due to the lower calorific value of biodiesel. They observed slightly higher brake thermal efficiency for SME, YGME and their blends. According to them the reason is—The oxygen-rich biodiesels promote a better combustion. The heat losses (all the heat losses together except exhaust loss) from the engine, when operated on SME and YGME were 4% and 3.1% higher than No. 2 diesel fuel, respectively. This was also attributed to the promotion of better combustion with the biodiesels. They also suggested to provide insulations for combustion chamber walls to reduce heat loss but consequently this will increase exhaust heat loss [39]. The biodiesels in this experiment exhibited lower exhaust loss compared to No. 2 diesel fuel. The reason they pronounced is—No. 2 diesel fuel operation deals with high HC and CO concentrations in the exhaust gas. The thermodynamic analysis of a single cylinder direct injection (DI) diesel engine operating on palm oil methyl ester (POME) was done by Debnath et al. [40]. POME has 5% lower calorific value than diesel fuel. So its thermal efficiency is lower than diesel. They investigated the effects of compression ratio and ignition timing on energy distribution. Compression ratio and ignition timing have some significant consequences on energy balance of the engine. At a compression ratio of 17.5 and 23° BTDC ignition timing, POME gives 9% lower brake thermal efficiency than diesel. At this compression ratio and ignition timing, the energy balance shows, 25% energy used as brake power, 30% energy is lost through the cooling water, 17% energy is lost with exhaust gas and the remaining portion is unaccounted for diesel fuel. At a CR of 16 and 28° BTDC ignition timing, POME gives higher brake power and lower unaccounted loss than the diesel fuel. Now the CR is 18 and for the same ignition timing (28° BTDC), POME gives higher brake power and less unaccounted loss than that of diesel fuel. The cooling water loss and exhaust loss increased in both cases. Advancement in ignition timing results higher heat release rate. It means that the fuel is supplied at cooler environment comparing with retardation. Hence, the fuel consumption rate increases more for the same amount of brake power. Advancement and retardation in ignition timing has increased the brake power hence the brake thermal efficiency for POME. This is because of the reduction of fuel supply. As the compression ratio increases, the less amount of fuel is required to input. It also increases the heat release rate during the combustion stroke. As a result, cooling water loss increases. At the same time lower exhaust temperature confirms lower exhaust loss with increasing CR. However, the unaccounted loss was unaffected at higher CRs. There were fluctuations in unaccounted heat loss for CR and ignition timing variations. Similar kinds of trends have been shown in case of another biodiesel Jatropha methyl ester (JME) [41]. They also suggested

for the retardation of the ignition timing. It works very effectively for LHR engines to recover the exhaust heat loss [42]. Another energy balance experiment using SME, YGME and SME with cetane improver 2-ethylexyl nitrate (EHN) was carried out by Tat [43]. The brake power were 40.23% for SME, 40.2% for SME with 0.75% (w/w) EHN, 40% for SME with 1.5% (w/w) EHN and 39.39% for YGME. The cooling water loss were 33.3% for SME, 33.6% for SME with 0.75% (w/w) EHN, 33.76% for SME with 1.5% (w/w) EHN and 33.62% for YGME. The exhaust loss were 26.37% for SME, 26.19% for SME with 0.75% (w/w) EHN, 26.2% for SME with 1.5% (w/w) EHN and 26.3% for YGME. The cetane number for SME was 50.4 and for YGME, it was 62.6. The brake power decreased with the increase of cetane number and consequently, the other losses increased. Similar results were found in case of Azoumah et al. [44] and Agudelo el al. [45] experiments. The lower cetane number lengthened the ignition delay period and caused more premixed combustion, which led to higher brake power due to the sudden rises in temperature and pressure in the combustion chamber. An experimental investigation by Benjumea et al. [46] has shown, neat palm oil biodiesel exhibits lower brake power and higher heat losses compared to diesel fuel (Table 3).

3.3. Energy balance using hydrogen fuel

Hydrogen has higher specific heat ratio ($\gamma = 1.4$) than gasoline fuel ($\gamma = 1.1$) due to its simpler molecular structure [59]. Hydrogen also has higher research octane number (RON), lower flammability limits and higher heating value than gasoline [60,61]. As a consequence, hydrogen engine has much more theoretical thermal efficiency than gasoline engine. The laminar burning velocity, propagation velocity and buoyant velocity of hydrogen are much higher than other fuels [62].

Yüksel and Ceviz [9] studied the energy balance of a four-cylinder (Ford MVH-418), four-stroke, SI engine using hydrogen as supplementary fuel with gasoline. They have shown that with the increase of engine load, the percentage of engine brake power decreased, while the unaccounted loss increased. Initially the increment was stiffer than the later stage because engine attains optimum operation at later stages [8,9]. Hydrogen supplementation significantly reduced the amount of heat loss to the cooling water by 36% of the mean average values. The unaccounted loss was also decreased by 30% of the mean average values. When pure gasoline was used, the heat loss to the cooling water was 16%, whereas it was 15, 13 and 12% for 0.129, 0.168 and 0.208 kg/h hydrogen supplementation, respectively. This happened because of the leaner combustion of hydrogen–gasoline with the help of auxiliary air entrance. The heat loss with the exhaust gasses was almost same compared to pure gasoline operation, because the exhaust gas temperature increased. For considerable amount of improvement in thermal efficiency in a CNG (compressed natural gas) fuelled SI engine, 5% to 7% hydrogen addition is necessary [54,63]. A comparative study between gasoline and hydrogen fuel in a research engine (single cylinder) at 2000 rpm has shown that hydrogen can give 6.42% higher thermal efficiency than gasoline engine. The reasons behind this are lower heat rejection and blow down during exhaust stroke, combustion near top dead centre (TDC) and isochoric combustion environment [50,64–66].

Dimopoulos et al. [15] investigated the energy balance of a SI engine using H_2–CNG mixture. The balance was done in terms of indicated thermal efficiency, incomplete combustion loss, actual combustion loss, wall heat loss, gas exchange loss, mechanical loss, real gas and blow-by loss. They observed the variations in energy balance by changing the percentage of exhaust gas recirculation (EGR) and H_2. Hydrogen addition accelerated the combustion process. The actual combustion loss decreased but the wall heat loss increased with hydrogen addition, while it left no

Table 3
Comparison among the conventional fuels and alternative fuels in terms of chemical and thermodynamic properties [41,43,46–58].

Property	Hydrogen	LPG	Methane	Gasoline	Diesel	Methanol	Ethanol	n-Butanol	POME	SME	YGME	JME
Chemical composition (%vol)	H_2	C_3H_8-30 C_4H_{10}-70	CH_4	C_8 H_{18}	$C_{12}H_{26}$	CH_3OH	C_2H_5OH	C_4H_9OH	$C_{18.07}H_{34.93}O_2$	$C_{18.74}H_{34.51}O_2$	$C_{18.4}H_{35.26}O_2$	~$C_{19}H_{34}O_2$
Molecular weight (g/mol)	2.016	53.87 (>44)	16.04	114.236	170	32	46	74	284.2	291.73	288.29	~294
Mass density (kg/m^3) at 1 atm and 15 °C	0.08	2.26	0.65	692	820–850	796	809.9	810	864–871.6	885	–	862–886
Kinematic viscosity (mm^2/s) at 40 °C	–	–	–	–	2.6	0.596	1.2	2.5	4.73	4.59	5.91	4.4–5.6
Boiling point(°C)	−252.8	−42-0	−161.4	37–205	180–360	66	79	118	348	–	–	–
Flashpoint (°C)	−231	-60	−188	-45	50–90	11	13	35	135	141–167	161	155
Minimum Ignition energy (MJ)	0.017	0.30	0.30	0.29	–	0.14	–	–	–	–	–	–
Flammability limits in air (%vol)	4.75	2.15	5–15	1.0–7.6	1.5–7.6	6–36.5	3.3–19	1.4–11.2	–	–	–	–
Auto ignition temperature in air (K)	858	678–723	723	533–733	527	737	696	–	–	–	–	–
Higher heating value (MJ/kg)	142	50.152	55.5	47.3	44.8	22.7	–	–	39.4	39.87	39.81	40.7
Lower heating value (MJ/kg)	120	45.7	50	43.8	42.5	20.27	26.8	33	37.13	33.5–37.38	37.14	38.5
Flame velocity in air (cm/s)	265–325	38.25	37–45	37–43	33	35	39	–	–	–	–	–
Stoichiometric air/fuel ratio (kg/kg)	34.2	15.5	17.1	14.6	15	6.66	9	11.2	12.5	–	–	–
Octane number (RON)	>130	103–105	125	95	30	108.7	108.6	–	–	–	–	–
Octane number (MON)	130	90–97	120	85	–	88.6	89.7	86	–	–	–	–
Cetane number (ASTM D613)	–	–	–	–	47.5	–	5–8	17–25	58–65.5	46–56	62.6	53–59

Table 4
Engine heat losses compared to theoretical engine cycle at 2000 rpm [14,15,67].

Load	IMEP, 2 bar			IMEP, 6 bar			BMEP, 2 bar			BMEP, 4 bar		
Fuel	Gasoline	H_2 PFI	H_2 DI	Gasoline	H_2 PFI	H_2 DI	CNG	CNG+10% vol. H_2	CNG+15% vol. H_2	CNG+8% EGR+0% vol. H_2	CNG+10% EGR+10% vol. H_2	CNG+12% EGR+15% vol. H_2
Efficiencies/losses [%]												
Indicated thermal efficiency	28.0	32.0	29.0	35.0	37.0	37.2	35.8	35.8	35.8	35.8	35.8	35.8
Incomplete combustion loss	2.0	9.0	12.0	1.0	0	0	5.8	4.5	6.6	6.3	4.5	5.8
Actual combustion loss	2.5	4	3	2	2	1.5	4.5	4.2	3.7	9.2	5.5	4.3
Wall heat loss	7.0	8	10	8	8	11	8.5	8.8	9.3	7.0	9.9	9.9
Gas exchange loss	8.0	2	1	2	1	1	5.9	5.9	5.9	5.9	5.4	5.0
Real gas, blow-by	–	–	–	–	–	–	8.5	9.2	6.8	5.2	6.9	6.8
Mechanical loss	–	–	–	–	–	–	11.0	11.1	11.3	11.5	11.3	11.5

IMEP = indicated mean effective pressure, BMEP = brake mean effective pressure, PFI = port fuel injection, DI = direct injection, EGR = exhaust gas recirculation.

effect on the gas exchange loss. The reduction in combustion loss is the witness of the accelerated combustion. The rapid burning rate of hydrogen rich CNG induced high in-cylinder temperature which increased the incomplete combustion loss. Later, due to the use of EGR, the combustion acceleration with the increase of hydrogen content was even more marked. The actual combustion loss of hydrogen rich CNG was dropped to 50% compared to pure CNG operation because 15% (vol.) hydrogen added CNG has the lowest late expansion temperatures [14,15]. Similar energy balance investigation was found in another literature [67]. They compared the results with gasoline fuel for two different H_2 injections: port fuel injection (PFI) and direct injection (DI). The results are tabulated (Table 4) for clear view. The ideal engine efficiency during the hydrogen operation was higher than gasoline due to the lean operation (i.e. higher A/F ratio and CR) of hydrogen. But lean operation of hydrogen resulted in higher incomplete combustion loss and actual combustion loss than gasoline. The wall heat loss was also higher during hydrogen operation, due to the high flame speed and small quenching distance. The gas exchange loss in hydrogen operation was very low compared to gasoline, due to the unthrottled operation of the engine [68]. Hydrogen engines are more docile to high speed engine operation due to the first burning rate of hydrogen [50]. During the intake stroke, the hydrogen injection prevents backfire but reduces output power and thermal efficiency due to knock produced by lower volumetric efficiency. During the compression stroke, the hydrogen injection prevents knock and increases output power and thermal efficiency. At the later stage of compression stroke, the hydrogen injection gives more than 38.9% thermal efficiency, 0.95 MPa BMEP and large amount of NO_x emission reduction [69].

3.4. Energy balance using LPG

The liquid petroleum gas or LPG has been used in both SI and CI engines as an alternative fuel [70,71]. Özcan and Söylemez [12] investigated the energy balance of a LPG fuelled SI engine which shows that 25%, 11.5%, 16.6% and 46.88% of the supplied fuel energy are distributed as brake power, cooling water loss, exhaust loss and unaccounted loss respectively at 1000 rpm. When the speed increased, the brake power, the cooling water loss and the exhaust loss were increased by 4.7%, 6.2% and 12.7%, respectively while the unaccounted loss was decreased by 23.7%. At higher rpm, due to the lower combustion period which means fewer time is available for convection and radiation heat transfer, the unaccounted loss decreased to a great extent. Hence the other losses were increased by a significant amount. In case of water injection, with the increase of water in LPG, the brake power and the unaccounted heat loss increased while the other losses decreased. For pure LPG operation, the water heat loss and the exhaust heat loss were 15% and 26% respectively, whereas it reduced to 14% and 23% respectively for 50% water injection. The average brake power and the unaccounted loss were 30% and 28% respectively for pure LPG operation, whereas it increased to 32% and 30% respectively for 50% water injection. The brake power increased with water addition because it lowered the temperature of the intake charge due to the supercharging effect which ensured more efficient combustion with respect to pure LPG. The cooling water loss decreased with the water addition because the overall in-cylinder temperature decreased. With the increase of water content in LPG, the exhaust gas temperature decreased which ensured lower exhaust loss. According to them, the more water is supplied to the engine, the more heat will be absorbed. At the same time, the water heat loss increased in a little amount as compared to the exhaust heat loss. But, finally both the water and exhaust heat loss decreased with respect to pure LPG. The unaccounted heat loss increased with water injection due to lower flame speed. The break thermal efficiency of the engine increased with water addition because of lower fuel consumption rate. Bayraktar and Durgun [71] reported that the LPG burns faster than gasoline which reduces heat loss to the cooling water but increases the exhaust loss.

4. Energy balance of LHR engines

The immense quests for increasing thermal efficiency of internal combustion engines have created momentum to make adiabatic engines by reducing energy losses. These engines are known as LHR engine or insulated engine or adiabatic engine. The energy balance of a 6-cylinder, DI, water-cooled and turbocharged diesel engine was investigated by Taymaz [10]. He compared the results of a standard engine (not coated) with an adiabatic engine (coated with the ceramic layer of $CaZrO_3$+$MgZrO_3$+NiCrAl). The results provided, indicate a clear reduction in heat loss to the cooling system and an increase in exhaust heat loss compared to standard engine though thermal efficiency is not increased to the same extent. The heat loss to the cooling system for standard engine were 49%, 36% and 27% for low (20%), medium (50%) and high (80%) loads respectively at 20° crank angle whereas these were decreased by 3%, 2% and 4% respectively for LHR engine. The heat loss with the exhaust gas of LHR engine for low, medium and high loads were 27%, 27% and 37% respectively and those are 3%, 4% and 8% higher than standard engine. The simple fact, acting behind the findings is the lower thermal conductivity of the ceramics. The ceramic insulation increases the engine combustion temperature; hence, the expansion work increases [72]. As a result, the brake power rises by 2% at medium load condition and by 1% at high load condition compared to standard engine. Similar results were found by another researcher, Ciniviz [73]. He has conducted a comparative energy balance analysis between standard diesel

engine and LHR engine operating on diesel and ethanol fuel. Compared to standard diesel engine, the coolant heat loss was decreased by 15% and 22% for diesel and ethanol fuel respectively, at 2800 rpm. He also reported that the reduced coolant heat, mostly lost as exhaust energy in LHR engine, at all speeds. Compared to standard diesel engine, the exhaust heat loss was increased by 11% when diesel fuel was used in LHR engine and decreased by 60% when ethanol fuel was used in LHR engine, at 1400 rpm. However, when the speed was doubled, the effects had been reduced (11% and 60% changed to 8% and 48%). The low thermal conductivity of the ceramics reduced the coolant heat loss. As a result, the combustion temperature hence the brake power was increased by 2% at medium load and by 1% at high load when the LHR engine was operated on diesel fuel. When ethanol fuel was used in LHR engine, the brake power decreased by 22.5%, at all speeds. Modi [74] studied the energy balance of a Partially Stabilized Zirconia (PSZ) coated diesel engine fuelled with diesel and biodiesel. The percentage of biodiesel (used in the experiment with diesel fuel) was not mentioned in the literature. However, the heat loss to the cooling water was decreased by 7%, 7% and 2% for high (80%), medium (50%) and low (20%) loads respectively compared to the uncoated engine. The exhaust heat loss was increased by 9%, 5% and 5% for high, medium and low loads, respectively compared to the uncoated engine. He mentioned that the volumetric efficiency of the engine decreased due to the rise in temperature of the inside wall, which is verified by Giakoumis [75] for two different coatings. The unaccounted loss decreased for the LHR engine, at all loads. Rajendra Prasath et al. [76] claimed 30% to 40% reduction in cooling water heat loss in a JME fuelled LHR engine. Hazar [77] has reported an improvement in the engine power by 8.4% and 1.6–3.5%, a reduction in fuel consumption by 4.9% and 4.7–8.0% and an increment in exhaust loss by 11.4% and 2.6–5.4% for No. 2 diesel fuel and canola methyl ester blended diesel fuels, respectively. He also conducted similar experiments in LHR engines using cotton methyl ester biodiesel along with No. 2 diesel fuel and the results were same [78,79]. Similar outcome also established while using pure vegetable oils in LHR engines and there were no anomalies after 100 h of the engine operation on the engine parts [80,81].

5. Theoretical investigation of energy balance

5.1. Multi-zone thermodynamic models

According to this thermodynamic model, fuel injection into the combustion chamber is divided into several zones. The cylinder pressure and the volumes of those zones are calculated by an ordinary differential equation (ODE) which has been developed by using the first law of thermodynamics, the ideal gas equation and other thermodynamic relations. The ODE is usually solved by Runge–Kutta (RK-4) method which will give cylinder pressure and zone volumes. The zone temperatures can be found by putting the engine cylinder pressure and zone volume into the ideal gas equation [11,20,25,82].

5.2. Energy balance using multi-zone models

Multi-zone models are generally used in diesel engines with light oil (gasoline, ethanol etc.) fumigation [11,82] and also diesel–ethanol blends [25]. These models have been satisfactorily applied to perform energy balance and various parametric analyses using light oil fumigation in diesel engines. Light oil fumigation is considered as an effective tool to reduce heat losses and increase brake power. According to the theoretical energy balance by Durgun and Şahin [11], at an average of 42% of the supplied fuel energy is converted to the indicated work for three different engines using neat diesel fuel, at all speeds; 30% and 27% of the supplied fuel are lost as exhaust and cooling loss, respectively. The brake power was increased by 1.98%, 3.64% and 5.72% for 2.5%, 5% and 7.5% gasoline oil fumigation with diesel fuel, respectively [11]. This happened due to the cooling effect of gasoline evaporation during the inlet process and also more efficient combustion compared to diesel fuel [19,82]. With the increase of fumigation ratios, the combustion duration increased, hence the wall heat loss increased. Consequently, the exhaust heat loss decreased with the increase of fumigation percentage. For small capacity spark ignition engines [34], a theoretical model has been developed by Wu et al. [83] based on Stanton number.

5.3. Single-zone thermodynamic models

In a single-zone model, it is assumed that the working fluid inside the engine makes a thermodynamic system. This system exchanges energy and mass with the surroundings where the energy released during the combustion process is calculated with the application of the first law of thermodynamics. In a two zone model the working fluid is divided into a burned and an unburned zone. The burned zone contains equilibrium products of combustion and unburned gas zone contains homogeneous mixture of air, fuel and residual gas. These zones are assumed as two distinct thermodynamic systems, which interact energy and mass between themselves and with their common surroundings. A single zone thermodynamic model is uncomplicated and very easy to apply for measuring the burning rate of fuel, fraction fuel burned, heat losses, heat release rate, indicated parameters, gas temperatures and other engine performance tools compared to multi-zone models [84–86]. The accuracy of these models relies on the accuracy of the computed temperature and pressure, locating of TDC and specific heat ratios (γ) [87]. Many investigations have been carried out to find an accurate γ [88,89]. Ghojel and Honnery [84] have developed a single zone thermodynamic model to use diesel-water emulsion as alternative fuel in a four-stroke, four-cylinder and water cooled diesel engine. The main input of this model is the estimated trace of the in-cylinder pressure versus crank angle which will be available from the combustion analyser of the tested engine. The assumptions made for this model are; fuel supply rate is equal to fuel burning rate, fuel follows the behaviour of ideal gas, cylinder control volume holds homogeneous combustion products for any crank angles and the dissociation of air–fuel ratio is ignored for specific heat ratio calculation. The cooling water heat loss and dissociation heat loss are calculated by using Wiebe's technique [90]. Total apparent heat release rate can be found by integrating the amount of heat released for each crank angle resolution. The released heat in the cylinder is used to increase internal energy and do external work. A considerable amount of this heat is lost to the cooling water through the cylinder walls and head during the combustion and expansion strokes. A small fraction is also lost due to the dissociation of the combustion products and incomplete chemical reactions. Total fuel burning rate is equal to the summation of all losses i.e. dissociation, wall heat loss, incomplete combustion loss, leakages etc. plus apparent heat release rate. The convection and radiation heat losses can be computed by using empirical correlations developed by Annand [16], Wochni [17], Hohenberg [18] or Eichelberg [31]. The radiation heat losses are often neglected in most cases, especially in diesel engines which may make these models inappropriate [17,84,91]. Some appropriate models for radiation heat loss calculation are developed by Callahan and Ryan [92] and Assanis and Heywood [93].

5.4. Outcome of the single-zone models

Ghojel and Honnery [84] developed a model to calculate heat release rate and heat transfer coefficient using Wiebe's [90] technique. Maximum value of heat transfer coefficient varies around 360° crank angle because the expansion stroke starts from 360°. A comparative study shows that the heat transfer coefficient varies in the range of 6000 to 7000 W/m^2 K for Hohenberg [18] correlation, 2500 to 3000 W/m^2 K for Woschni [17] correlation and 1500 to 1800 W/m^2 K for Annand [16] correlation for a particular engine. This huge difference in coefficients is due to the negligence of radiation heat transfer coefficient in some cases and variations lie in assumptions during construction of those correlations. Ghojel et al. [91] investigated a heat release model using diesel water emulsion (13% H_2O by vol.). They found higher brake thermal efficiency but much higher BSFC for water emulsion. The brake thermal efficiency was increased in the range of 1% to 3% while using diesel–water emulsion instead of diesel fuel. The brake specific fuel consumption also increased in the range of 7–26% while others reported a decrease in BSFC [91,94–98].

6. The effects of the engine operating parameters and design factors on energy balance

Yamin and Badran [99] analytically studied the effects of the engine design factors and operating parameters on the percentage of heat losses in a SI engine operating on propane fuel. Heat losses from the internal combustion engines depend on many operating parameters and engine design factors like ignition timing, compression ratio, air–fuel equivalence ratio (λ), spark plug location (XSP), engine speed, flame speed, valve diameter, valve lift etc. They found, some factors like higher compression ratio, spark plug location near centre, larger valve area and leaner air–fuel equivalence ratio are in the favour of reducing heat loss. The summaries of their analyses are given in Table 5. The effects of the combustion chamber design factors on energy balance in three different types of SI engines have been investigated by Mukai et al. [100]. They have considered swirl, squish and also the cylinder head material as variables for their investigation. They observed the influences of these factors on the engine brake power, the cooling loss and the exhaust loss. They divided the cooling heat loss into the cylinder head cooling loss (Q_h) and the cylinder block cooling loss (Q_b). The large portion (65%) was lost in the block side. The gas flow by swirl propagated through the entire combustion chamber and the heat transfer to the cylinder wall was promoted. The Swirl, in the combustion chamber, was generated by decreasing (35%) the area of the guide pipe of air–fuel mixture in the inlet port. The gas flow by squish was in a direction along the head wall surface at TDC and the effects were seem to be small compared to swirl. The intensity of the squish was changed by reducing the area of squish about 15%. The cylinder head and bore are usually made of aluminium alloy and cast iron, respectively. The aluminium alloy has a thermal expansion coefficient 80% higher than cast iron [101]. They replaced the 10 mm thick aluminium alloy cylinder head with 5 mm thick cast iron (combustion chamber side) plus 5 mm thick aluminium alloy. As a result, the combustion chamber temperature increased by about 40 °C due to the low thermal

Table 5
The effects of the engine design factors and operating parameters on heat losses [99].

Parameters	Trends of the parameters	Engine condition during operation					% heat losses[b]	Remarks
		Speed (rpm)	CR	Λ	XSP[a]	Throttle position and spark timing		
Spark timing	Advancing	2000	9.0	0.7–1.2	0.395	WOT[c]	Increases	Due to the completion of combustion within TDC (more time available for heat losses).
Compression ratio	Increasing	2000	N/A	1.0	all	WOT and MBT[d]	Increases	Due to the increase of in–cylinder temperature and also the completion of combustion near TDC.
Spark plug location (XSP)	Shifting from edge towards the centre	2000	≤ 9.0					– Due to the reduction in flame travel path. – Valid up to 9.0 CR because knock increases drastically after this point.
Speed	Increasing	N/A	9.0	0.7–1.2	0.395	WOT and MBT	Decreases	– Lower combustion duration – 0.395 is chosen because engines show good performances at this position.
Air-fuel equivalence ratio (λ)	$\lambda \leq 1$ $\lambda > 1$	2000	9.0	N/A	0.395	WOT and MBT	Increases Decrea-ses	– Rich mixture causes high enthalpy of combustion. – Lean mixture causes poor combustion.
Inlet valve diameter and lift	Increasing	2000	9.0	0.7–1.2	0.395	WOT and MBT	Decreases	– Due to the availability of more fresh mixture. – Valve diameter enlargement is recommended. – Valve lift increment can make noisier engine operation.
Combustion duration	Increasing	1000–3000	9.0	0.7–1.2	0.395	WOT and MBT	Increases	Due to the more available time for heat losses to the surroundings.
Flame speed	Decreasing	1000–3000	9.0	0.7–1.2	0.395	WOT and MBT	Increases	– Combustion products have more available time to reject heat to the surroundings. – This trend is dominating at lower RPM due to the low turbulence.

[a] Ratio of spark plug position from the nearest wall to cylinder bore.
[b] Heat losses to the engine surroundings.
[c] Wide open throttle.
[d] Maximum brake torque.

Table 6
The effects of the combustion chamber design factors on the heat balance of SI engines, rpm = 1600, A/F = 16.6 and 50% charging rate [100].

Combustion chamber design factors	Variable	Combustion chamber shape	Brake power	Cooling loss		Exhaust loss	Remarks
				Head side	Block side		
Swirl	Strengthened	Hemispherical	Increased a little	Increased	Increased	Decreased	– Turbulence occurs in the combustion chamber due to swirl which accelerates the burning speed. – High burning speed increases engine thermal efficiency and consequently the brake power increases. – Due to the rise in gas motion, heat transfer co-efficient increases which accelerates the cooling losses. – Cooling losses also increase due to the large expansion period.
Squish	Weakened	Wedge	Decreased a little	Decreased	No changes	Increased	Gas flow is weakened by making the squish area small. As a result, cooling losses decrease.
Cylinder head material	Changed to 5 mm Al+5 mm CI	Rugged hemispherical	No changes	Decreased	Almost equal	Increased	– Low thermal conductivity of the cast iron reduces the cylinder head side cooling losses. – The amount saved from cooling losses is lost with the exhaust gasses leaving no impact on brake power.

conductivity of the cast iron [102]. The findings of their investigation are tabulated (Table 6).

Colaço et al. [103] conducted experiment to measure piston side heat loss by varying the piston material using diesel, palm oil biodiesel and their blends. They reported, due to the high thermal conductivity and diffusivity, the temperature gradient was not very pronounced in the piston while using aluminium alloy. So the thermal stress was not very high, but in case of cast iron piston, higher variation of temperature was noticed. Jafari and Hannani [104] reported, higher CR reduces heat loss to the cooling systems. They also found, a change in the equivalence ratio from 1.2 to 1.0 reduces heat loss, retardation of the spark timing results in a decrease in the heat loss and higher swirl ratio increases the heat loss to the cylinder walls. The reasons are, higher CR makes combustion faster, spark timing retardation results in lower mixture temperature and bulk pressure in the cylinder and higher swirl ratio causes higher gas velocity and better mixing. The peak heat flux occurs at an equivalence ratio of 1.1 and a dilution or enrichment from this value reduces heat loss to the cylinder walls.

7. The roles of turbocharger and supercharger on energy balance

The maximum power that an engine can deliver is limited by the amount of fuel that can be burned efficiently inside the cylinder. This is also limited by the amount of air that is introduced into each cylinder during each cycle. If the induced air is compressed to a higher density than ambient condition, prior to entry into each cylinder, the maximum power delivered by the engine will be increased. The primary purpose of turbocharging and supercharging is to increase the air density by increasing its pressure prior to entering the cylinder. In turbocharging process, a turbocharger (i.e. a compressor and a turbine on a single shaft) takes energy from the exhaust stream to drive the turbine which drives the turbocharger compressor to boost the inlet air density. In supercharging process, a separate pump, compressor or blower takes power from the engine drive shaft to provide the compressed air prior to entry to each engine cylinder. Turbo-compounding (i.e. use of 2nd turbine in the exhaust), two stage turbocharging, turbocharging with after cooler or inter cooler (i.e. charge cooling with a heat exchanger after compression) are some improved versions of turbocharging and supercharging to increase the air density more [5,6].

The following examples will help to understand the importance to study the effects of these devices on energy balance. A turbocharged CI engine can give 33% higher power and 46% higher torque than a naturally aspirated CI engine. The use of turbocharger and supercharger in SI engines is limited by knock. However, a turbocharged SI engine gives 15 kW more power at 5400 rpm and 26 N m more torque at 3800 rpm than a naturally aspirated SI engine. A turbocharged and after-cooled SI engine gives 34 kW more power at 5300 rpm and 66 N m more torque at 2900 rpm than a naturally aspirated SI engine. The BSFC of a typical turbocharged, direct injected, diesel engine is 5–6% lower than the naturally aspirated one. It is possible to reduce another 5–6% BSFC by adding after-cooler and it can be further reduced by another 5–6% if we use turbo-compounding system [5]. An energy balance shows, 5.86% of the supplied fuel energy is lost through the turbocharger in a six-cylinder, turbocharged and after cooled CI engine operating at 224 kW and 2100 rpm [105]. All the researchers who investigated the effects of various parameters associated with turbocharging on engine performance agreed that the turbocharging is a successful way to improve thermal efficiency as the engine combustion is more complete now and the exhaust heat loss is reduced [6,38,46,103,105]. At present, the majority of the CI engines are equipped with turbocharger and after cooler [5].

So the energy balance of a turbocharged or supercharged engine will be different from a naturally aspirated one in the sense that the subsystems (i.e. turbocharger, after-cooler, supercharger etc.) also require energy balance. It is possible by calculating the enthalpy differences across these subsystems. The turbine of the turbocharger extracts heat energy from the exhaust gas by an expansion process. Some of this energy is dissipated as mechanical losses in the bearings and then appears as heat to the lubricating oil. The turbine volute also rejects heat directly to the surrounding cooling medium. A fraction of the compressor power appears as charge heating and some of the compressor work assists in reducing engine pumping work and hence appears as indicated engine power. A large fraction of the indicated work survives as brake power whilst the remainder is dissipated to the lubricating oil and cooling medium or is used to drive ancillaries such as fuel injection pump, lubricating pump and water pump [106,107]. So it is clear that the coolant heat loss and lubricating oil heat loss will increase, exhaust heat loss will decrease and brake power will increase if we use turbocharger or supercharger in a naturally aspirated engine.

A theoretical investigation of energy balance among two turbocharged (one is Ottikkutti's engine [108] and other one is Li's engine [109]) and one naturally aspirated (from Gupta [110]) diesel engines has given by Durgun and Şahin [11]. As expected, the brake power is much higher for both turbocharged engines than the naturally

aspirated one. The exhaust heat loss was around 30% for both turbocharged engines and 35% for naturally aspirated one, which is a clear indication of exhaust heat loss reduction. Consequently, the coolant heat loss or wall heat loss is increased slightly due to the increased in-cylinder heat transfer by turbocharging action [6,11]. According to their reports, the energy balance scenario is same in case of gasoline fumigation with diesel fuel for those engines. Canakci and Hosoz [38] have performed energy balance on a 4-cylinder, turbocharged John Deere 4276 T type diesel engine using SME and YGME. Both biodiesels showed higher BSFC which is already explained in Section 3.2, but the heat loss characteristics showed expected results. The coolant heat loss was much higher than the exhaust heat loss and the brake power improved a lot due to the turbocharging effect. McCarthy et al. [111] investigated two 4-cylinder, indirect injection diesel engines; one is naturally aspirated and another one is turbocharged using various biodiesels. They reported a decrease in power and torque (4–5%) while using biodiesels due to higher heat losses through the cooling medium despite the use of turbocharger. The reasons are already explained in the Section 3.2. Other research groups [46,62,103] also found similar results for turbocharged or supercharged engines while using biodiesels. As the coolant heat loss increases in turbocharged engine, many researchers [39,73,75,112,113] tried to reduce this loss by insulating the combustion chamber with lower conductivity ceramic materials (i.e. LHR engines). In LHR engines, the coolant heat loss reduces and hence the exhaust heat loss increases which means more available energy in the turbine blade of the turbocharger. Giakoumis [75] reported an increase of 2.4% brake power due to the applied insulation in the combustion chamber of a turbocharged engine. The above roles of turbocharger and supercharger on energy balance are also supported from the second law of thermodynamics point of view [6,38,105,114,115].

8. Conclusions

A comprehensive survey on the energy balance of IC engines using alternative fuels is presented in this literature. Extensive theory on the energy balance is given including the application of the first-law of thermodynamics, variations in heat transfer correlations for wall heat loss evaluation, thermodynamic models etc. This literature covered all the alternative fuels for energy balance analysis along with most of the engine variable's effects on the energy balance. The latter one can be a very useful material for the designers since it identifies which particular parameters have the most significant effects on the engine performance. This is the first and inclusive review on the research progress made in the energy balance analysis of internal combustion engines.

The following conclusions are drawn based on the literature surveyed:

- Hohenberg's correlation is the best suited equation for SI engine.
- Heat loss reduces by a significant amount when the percentage of alcohols in the blend is greater than fifteen.
- Biodiesels have lower thermal efficiency than diesel fuel. For same amount of output power, the BSFC of biodiesels is much higher than diesel fuel. The heat losses except the exhaust loss are higher while using biodiesels due to the presence of excessive oxygen molecules. Thermal insulation can be a good solution in this regard; meanwhile it will increase the exhaust heat loss. The brake power decreases with the increase of cetane number. The cooling water loss is comparatively higher than the exhaust heat loss for biodiesels.
- Hydrogen supplementation with gasoline fuel significantly reduces the cooling water loss. Hydrogen addition in CNG reduces the actual combustion loss, increases the incomplete combustion loss, increases the wall heat loss and leaves no effect on the gas exchange loss. The lean operation of hydrogen increases the incomplete combustion loss and the complete combustion loss compared to gasoline fuel.
- LPG burns faster than gasoline. Water addition in LPG has a favourable effect on reducing heat losses compared to pure LPG operation.
- The cooling water loss is very much lower in LHR engines for all alternative fuels compared to any other engines due to the low thermal conductivity of the insulations. The brake power increased in the range 1–3% at any loading conditions in LHR engines.
- The single-zone thermodynamic models are comparatively easier to apply and exhibit reasonable accuracy but for better accuracy multi-zone models are preferable.
- Large inlet valve and lift, retarding spark timing, CR around nine, air-fuel equivalence ratio less than one, spark plug location near centre are in the favour of reducing heat loss to the engine surroundings in a LPG operated SI engine. A large portion of the cooling loss is lost in the cylinder block side. Higher swirl and squish ratio accelerate the cooling heat loss. Cylinder head material with lower conductivity lowers the head side cooling heat loss and does not affect the block side cooling heat loss.
- Turbochargers boost the inlet air density by extracting energy from the engine exhaust with the help of a turbine and a compressor. As a result, the exhaust heat loss decreases whilst the coolant heat loss and the brake power increase. Like turbocharging, supercharging has similar effects on energy balance.

From the conducted review of the published works on IC engine energy balance using alternative fuels, the following interesting research gaps are identified:

Most important requirement for IC engine energy balance is a suitable heat transfer correlation. The existing correlations are based on diesel engine experiments using diesel fuel. But the combustion and heat release characteristics of alternative fuels are different from diesel fuel due to the variations in fuel chemical compositions. So the heat transfer correlations need to be adjusted according to a particular fuel such as ethanol, biodiesel through experiments to predict more accurate heat losses. Along with this, investigations should be carried out to find a new heat transfer correlations considering more variables and all modes of engine heat transfer. Though lots of investigations have been done for heat transfer modelling but still there is a need of better and easily applicable model. Energy balance on industrial or marine engines under transient operation can be a good research subject as these engines are characterized by different combustion systems, lower rotational speeds, lower swirl ratios and greater dimensions, all of which might influence the heat loss patterns. Intense investigation on energy balance under fundamental discrete transient schedules (acceleration, cold starting and increasing loads) is required to reveal the feasibility of the alternative fuel blends in IC engines. Energy balance using alternative combustion technologies such as PCCI and HCCI is worthy of investigation.

Acknowledgments

The authors would like to acknowledge University of Malaya, Kuala Lumpur, Malaysia for financial support through High Impact Research Grant entitles: “Clean Diesel Technology for Military and Civilian Transport Vehicles” Grant no. UM.C/HIR/MOHE/ENG/07.

References

[1] Ong H, Mahlia T, Masjuki H. A review on energy pattern and policy for transportation sector in Malaysia. Renewable and Sustainable Energy Reviews 2011.

[2] Masum B, Masjuki H, Kalam M, Rizwanul Fattah I, Palash M, S, et al. Effect of ethanol–gasoline blend on NO_x emission in SI engine. Renewable and Sustainable Energy Reviews 2013;24:209–22.

[3] Arbab MI, Masjuki HH, Varman M, Kalam MA, Imtenan S, Sajjad H. Fuel properties, engine performance and emission characteristic of common biodiesels as a renewable and sustainable source of fuel. Renewable and Sustainable Energy Reviews 2013;22:133–47.

[4] Martyr A, Plint MA. Engine testing: theory and practice. Butterworth-Heinemann; 201–10.

[5] Heywood JB. Internal combustion engine fundamentals. McGraw-Hill Book Company; 668–701.

[6] Rakopoulos C, Giakoumis E. Second-law analyses applied to internal combustion engines operation. Progress in Energy and Combustion Science 2006;32:2–47.

[7] Moran MJ, Shapiro HN, Boettner DD, Bailey M. Fundamentals of engineering thermodynamics. Wiley; 2010.

[8] Ajav E, Singh B, Bhattacharya T. Thermal balance of a single cylinder diesel engine operating on alternative fuels. Energy conversion and management 2000;41:1533–41.

[9] Yüksel F, Ceviz M. Thermal balance of a four stroke SI engine operating on hydrogen as a supplementary fuel. Energy 2003;28:1069–80.

[10] Taymaz I. An experimental study of energy balance in low heat rejection diesel engine. Energy 2006;31:364–71.

[11] Durgun O, Şahin Z. Theoretical investigation of heat balance in direct injection (DI) diesel engines for neat diesel fuel and gasoline fumigation. Energy Conversion and Management 2009;50:43–51.

[12] Özcan H, Söylemez M. Thermal balance of a LPG fuelled, four stroke SI engine with water addition. Energy conversion and management 2006;47:570–81.

[13] Yildirim D, Ozgener L. Thermodynamics and exergoeconomic analysis of geothermal power plants. Renewable and Sustainable Energy Reviews 2012;16:6438–54.

[14] Dimopoulos P, Bach C, Soltic P, Boulouchos K. Hydrogen–natural gas blends fuelling passenger car engines: combustion, emissions and well-to-wheels assessment. International Journal of Hydrogen Energy 2008;33:7224–36.

[15] Dimopoulos P, Rechsteiner C, Soltic P, Laemmle C, Boulouchos K. Increase of passenger car engine efficiency with low engine-out emissions using hydrogen–natural gas mixtures: a thermodynamic analysis. International Journal of Hydrogen Energy 2007;32:3073–83.

[16] Annand WJD. Heat transfer in the cylinders of reciprocating internal combustion engines. Proceedings of the Institute of Mechanical Engineers 1963;177:973–90.

[17] Woschni G. A universally applicable equation for the instantaneous heat transfer coefficient in the internal combustion engine. SAE Transactions 1967;76:3065–83.

[18] Hohenberg GF. Advanced approaches for heat transfer calculations, SAE paper 790825, SP-449, 1979.

[19] Şahin Z, Durgun O. Theoretical investigation of effects of light fuel fumigation on diesel engine performance and emissions. Energy Conversion and Management 2007;48:1952–64.

[20] Şahin Z, Durgun O. Multi-zone combustion modeling for the prediction of diesel engine cycles and engine performance parameters. Applied Thermal Engineering 2008;28:2245–56.

[21] Ramadhas A, Jayaraj S, Muraleedharan C. Theoretical modeling and experimental studies on biodiesel-fueled engine. Renewable Energy 2006;31: 1813–1826.

[22] Rakopoulos C, Rakopoulos D, Giakoumis E, Kyritsis D. Validation and sensitivity analysis of a two zone diesel engine model for combustion and emissions prediction. Energy Conversion and Management 2004;45:1471–95.

[23] Liu Y, Reitz R. Modeling of heat conduction within chamber walls for multidimensional internal combustion engine simulations. International Journal of Heat and Mass Transfer 1998;41:859–69.

[24] Kumar S, Kumar Chauhan M. Numerical modeling of compression ignition engine: a review. Renewable and Sustainable Energy Reviews 2013;19:517–30.

[25] Rakopoulos C, Antonopoulos K, Rakopoulos D, Hountalas D. Multi-zone modeling of combustion and emissions formation in DI diesel engine operating on ethanol–diesel fuel blends. Energy Conversion and Management 2008;49:625–43.

[26] Rakopoulos C, Hountalas D. Development of new 3-D multi-zone combustion model for indirect injection diesel engines with a swirl type prechamber. SAE Technical Paper 2000-01-0587. 2000.

[27] Pulkrabek WW. Engineering fundamentals of the internal combustion engine. 2nd ed. Upper Saddle River, NJ, USA: Pearson Prentice-Hall; 2004.

[28] Alasfour F. Butanol—a single-cylinder engine study: availability analysis. Applied Thermal Engineering 1997;17:537–49.

[29] Boulahlib M, Boukebbab S, Gaci F, Kholai O. Experimental study of energy balance for air-cooled DI diesel engines operating in hot climates. SAE Technical Paper 2009-01-1974, 2009, http://dx.doi.org/104271/2009-01-1974.

[30] Lounici MS, Loubar K, Balistrou M, Tazerout M. Investigation on heat transfer evaluation for a more efficient two-zone combustion model in the case of natural gas SI engines. Applied Thermal Engineering 2011;31:319–28.

[31] Eichelberg G. Some new investigations on old combustion engine problems. Engineering 1939;148:463–547.

[32] Sitkei G, Ramanaiah GV. A rational approach for calculation of heat transfer in diesel engines. SAE technical paper 720027; 1972.

[33] Shayler P, May S, Ma T. The determination of heat transfer from the combustion chambers of SI engines. SAE technical paper 931131; 1993.

[34] Wu YY, Chen BC, Hsieh FC. Heat transfer model for small-scale air-cooled spark-ignition four-stroke engines. International Journal of Heat and Mass Transfer 2006;49:3895–905.

[35] Irimescu A. Study of cold start air–fuel mixture parameters for spark ignition engines fueled with gasoline–isobutanol blends. International Communications in Heat and Mass Transfer 2010;37:1203–7.

[36] Caton JA. Implications of fuel selection for an SI engine: results from the first and second laws of thermodynamics. Fuel 2010;89:3157–66.

[37] Abu-Zaid M, Badran O, Yamin J. Effect of methanol addition on the performance of spark ignition engines. Energy & Fuels 2004;18:312–5.

[38] Canakci M, Hosoz M. Energy and exergy analyses of a diesel engine fuelled with various biodiesels. Energy Sources, Part B 2006;1:379–94.

[39] Parlak A, Yasar H, Eldogan O. The effect of thermal barrier coating on a turbo-charged diesel engine performance and exergy potential of the exhaust gas. Energy Conversion and Management 2005;46:489–99.

[40] Debnath BK, Sahoo N, Saha UK. Thermodynamic analysis of a variable compression ratio diesel engine running with palm oil methyl ester. Energy Conversion and Management 2013;65:147–54.

[41] Kannan D, Pachamuthu S, Nurun Nabi M, Hustad JE, Løvås T. Theoretical and experimental investigation of diesel engine performance, combustion and emissions analysis fuelled with the blends of ethanol, diesel and jatropha methyl ester. Energy Conversion and Management 2012;53:322–31.

[42] Parlak A. The effect of heat transfer on performance of the diesel cycle and exergy of the exhaust gas stream in a LHR Diesel engine at the optimum injection timing. Energy Conversion and Management 2005;46:167–79.

[43] Tat ME. Cetane number effect on the energetic and exergetic efficiency of a diesel engine fuelled with biodiesel. Fuel Processing Technology 2011;92:1311–21.

[44] Azoumah Y, Blin J, Daho T. Exergy efficiency applied for the performance optimization of a direct injection compression ignition (CI) engine using biofuels. Renewable Energy 2009;34:1494–500.

[45] Agudelo J, Gutiérrez E, Benjumea P. Experimental combustion analysis of a HSDI diesel engine fuelled with palm oil biodiesel–diesel fuel blends. Dyna 2009;76:103–13.

[46] Benjumea P, Agudelo J, Agudelo A. Effect of altitude and palm oil biodiesel fuelling on the performance and combustion characteristics of a HSDI diesel engine. Fuel 2009;88:725–31.

[47] Canakci M, Ozsezen AN, Alptekin E, Eyidogan M. Impact of alcohol–gasoline fuel blends on the exhaust emission of an SI engine. Renewable Energy 2013;52:111–7.

[48] Khaliq A, Trivedi SK, Dincer I. Investigation of a wet ethanol operated HCCI engine based on first and second law analyses. Applied Thermal Engineering 2011;31:1621–9.

[49] Sayin C. Engine performance and exhaust gas emissions of methanol and ethanol–diesel blends. Fuel 2010;89:3410–5.

[50] Fayaz H, Saidur R, Razali N, Anuar F, Saleman A, Islam M. An overview of hydrogen as a vehicle fuel. Renewable and Sustainable Energy Reviews 2012;16:5511–28.

[51] Abbasi T, Abbasi S. 'Renewable' hydrogen: prospects and challenges. Renewable and Sustainable Energy Reviews 2011;15:3034–40.

[52] Mazloomi K, Gomes C. Hydrogen as an energy carrier: prospects and challenges. Renewable and Sustainable Energy Reviews 2012;16:3024–33.

[53] Rizwanul Fattah I, Masjuki H, Liaquat A, Ramli R, Kalam M, Riazuddin V. Impact of various biodiesel fuels obtained from edible and non-edible oils on engine exhaust gas and noise emissions. Renewable and Sustainable Energy Reviews 2013;18:552–67.

[54] Porpatham E, Ramesh A, Nagalingam B. Effect of hydrogen addition on the performance of a biogas fuelled spark ignition engine. International Journal of Hydrogen Energy 2007;32:2057–65.

[55] Hoekman SK, Broch A, Robbins C, Ceniceros E, Natarajan M. Review of biodiesel composition, properties, and specifications. Renewable and Sustainable Energy Reviews 2011.

[56] Mofijur M, Masjuki H, Kalam M, Hazrat M, Liaquat A, Shahabuddin M, et al. Prospects of biodiesel from Jatropha in Malaysia. Renewable and Sustainable Energy Reviews 2012;16:5007–20.

[57] Kalam M, Ahamed J, Masjuki H. Land availability of Jatropha production in Malaysia. Renewable and Sustainable Energy Reviews 2012;16:3999–4007.

[58] Jayed M, Masjuki H, Kalam M, Mahlia T, Husnawan M, Liaquat A. Prospects of dedicated biodiesel engine vehicles in Malaysia and Indonesia. Renewable and Sustainable Energy Reviews 2011;15:220–35.

[59] Wang S, Ji C, Zhang B, Liu X. Performance of a hydroxygen-blended gasoline engine at different hydrogen volume fractions in the hydroxygen. International Journal of Hydrogen Energy 2012.

[60] White C, Steeper R, Lutz A. The hydrogen-fueled internal combustion engine: a technical review. International Journal of Hydrogen Energy 2006;31:1292–305.

[61] Subramanian V, Mallikarjuna J, Ramesh A Performance, emission and combustion characteristics of a hydrogen fueled SI engine—an experimental study. SAE Technical Paper 2005-26-349. 2005.

[62] Lata D, Misra A. Theoretical and experimental investigations on the performance of dual fuel diesel engine with hydrogen and LPG as secondary fuels. International Journal of Hydrogen Energy 2010;35:11918–31.

[63] Das LM, Polly M Experimental evaluation of a hydrogen added natural gas (HANG) operated SI engine. SAE Paper No 2005-26-029.
[64] SinghYadav V, Soni S, Sharma D. Performance and emission studies of direct injection CI engine in duel fuel mode (hydrogen–diesel) with EGR. International Journal of Hydrogen Energy 2012;37:3807–17.
[65] Nieminen J, D'Souza N, Dincer I. Comparative combustion characteristics of gasoline and hydrogen fuelled ICEs. International Journal of Hydrogen Energy 2010;35:5114–23.
[66] Aleiferis P, Rosati M. Flame chemiluminescence and OH LIF imaging in a hydrogen-fuelled spark-ignition engine. International Journal of Hydrogen Energy 2011.
[67] Verhelst S, Wallner T. Hydrogen-fueled internal combustion engines. Progress in Energy and Combustion Science 2009;35:490–527.
[68] Moreno F, Muñoz M, Arroyo J, Magén O, Monné C, Suelves I. Efficiency and emissions in a vehicle spark ignition engine fueled with hydrogen and methane blends. International Journal of Hydrogen Energy 2012.
[69] Mohammadi A, Shioji M, Nakai Y, Ishikura W, Tabo E. Performance and combustion characteristics of a direct injection SI hydrogen engine. International Journal of Hydrogen Energy 2007;32:296–304.
[70] Thring R Alternative fuels for spark-ignition engines. SAE technical paper 831685; 1983.
[71] Bayraktar H, Durgun O. Investigating the effects of LPG on spark ignition engine combustion and performance. Energy Conversion and Management 2005;46:2317–33.
[72] Taymaz I, Mimaroglu A, Avcı E, Uçar V, Gur M. Comparison of thermal stresses developed in Al_2O_3–SG, ZrO_2–(12% Si+Al) and ZrO_2–SG thermal barrier coating systems with NiAl, NiCrAlY and NiCoCrAlY interlayer materials subjected to thermal loading. Surface and Coatings Technology 1999;116–119:690–3.
[73] Ciniviz M. Performance and energy balance of a low heat rejection diesel engine operated with diesel fuel and ethanol blend. Transactions of the Canadian Society for Mechanical Engineering 2010;34:93.
[74] Modi A Experimental study of energy balance in thermal barrier coated diesel engine. SAE technical paper 2012-01-0389; 2012, http://dx.doi.org/104271/2012-01-0389.
[75] Giakoumis E. Cylinder wall insulation effects on the first-and second-law balances of a turbocharged diesel engine operating under transient load conditions. Energy Conversion and Management 2007;48:2925–33.
[76] Rajendra Prasath B, Tamilporai P, Shabir MF. Analysis of combustion, performance and emission characteristics of low heat rejection engine using biodiesel. International Journal of Thermal Sciences 2010;49:2483–90.
[77] Hazar H. Effects of biodiesel on a low heat loss diesel engine. Renewable Energy 2009;34:1533–7.
[78] Hazar H. Cotton methyl ester usage in a diesel engine equipped with insulated combustion chamber. Applied Energy 2010;87:134–40.
[79] Hazar H. Characterization and effect of using cotton methyl ester as fuel in a LHR diesel engine. Energy Conversion and Management 2011;52:258–63.
[80] Aydin H. Combined effects of thermal barrier coating and blending with diesel fuel on usability of vegetable oils in diesel engines. Applied Thermal Engineering 2012.
[81] İşcan B, Aydın H. Improving the usability of vegetable oils as a fuel in a low heat rejection diesel engine. Fuel Processing Technology 2012;98:59–64.
[82] Şahin Z, Durgun O. High speed direct injection (DI) light-fuel (gasoline) fumigated vehicle diesel engine. Fuel 2007;86:388–99.
[83] Wu YY, Chen BC, Hsieh FC, Ke CT. Heat transfer model for small-scale spark-ignition engines. International Journal of Heat and Mass Transfer 2009;52: 1875–1886.
[84] Jamil Ghojel Dh. Heat release model for the combus-tion of diesel oil emulsions in DI diesel engines. Applied Thermal Engineering 2005;25: 2072–2085.
[85] Abd Alla GH, Soliman HA, Badr OA, Abd Rabbo MF. Combustion quasi-two zone predictive model for dual fuel engines. Energy Conversion and Management 2001;42:1477–98.
[86] Lakshminarayanan PA, Aghav YV, Dani AD, Mehta PS. Accurate prediction of the heat releasen in a modern direct injection diesel engine. Proceedings of the Institute of Mechanical Engineers 2002;216:663–75.
[87] Lapuerta M, Armas O, Bermúdez V. Sensitivity of diesel engine thermodynamic cycle calculation to measurement errors and estimated parameters. Applied Thermal Engineering 2000;20:843–61.
[88] Lapuerta M, Hernández JJ, Armas O Kinetic modelling of gaseous emissions in a diesel engine. SAE technical paper 2000-01-2939; 2000, http://dx.doi.org/104271/2000-01-2939.
[89] Ghojel JI. Computer time reduction in first law analysis of combustion systems. In: Proceedings international conference on fluid and thermal energy conversion' 94; 1994. vol 1, p 335–342.
[90] Wiebe II. New insight into the engine cycle (in Russian). Mashgiz, Moscow; 1962. Chapter 2, p. 35–89.
[91] Ghojel J, Honnery D, Al-Khaleefi K. Performance, emissions and heat release characteristics of direct injection diesel engine operating on diesel oil emulsion. Applied Thermal Engineering 2006;26:2132–41.
[92] Callahan TJ, Ryan TW Acquisition and interpretation of diesel engine heat release data. SAE paper 852068; 1985.
[93] Assanis DN, Heywood JB Development and use of computer simulation of the turbocharged diesel system for engine performance and component heat transfer studies. SAE paper 860329; 1986.
[94] Samec N, Kegl B, Dibble RW. Numerical and experimental study of water/oil emulsified fuel combustion in a diesel engine. Fuel 2002;81:2035–44.
[95] Barnaud F, Schmelzle P, Schulz P AQUAZOLE: an original emulsified water-diesel fuel for heavy-duty applications. SAE paper no 2000-01-1861; 2000.
[96] Abu-Zaid M. Performance of single cylinder, direct injection diesel engine using water fuel emulsions. Energy Conversion and Management 2004;45:697–705.
[97] Park J, Huh K, Lee J. Reduction of NOx, smoke and brake specific fuel consumption with optimal injection timing and emulsion ratio of water-emulsified diesel. Proceedings of the Institution of Mechanical Engineers, Part D: Journal of Automobile Engineering 2001;215:83–93.
[98] Barnes A, Duncan D, Marshall J, Psaila A, Chadderton J, Eastlake A Evaluation of water-blend fuels in a city bus and an assessment of performance with emission control devices. SAE technical paper 2000-01-1915; 2000, http://dx.doi.org/104271/2000-01-1915.
[99] Yamin J, Badran O. Analytical study to minimise the heat losses from a propane powered 4-stroke spark ignition engine. Renewable Energy 2002;27:463–78.
[100] Mukai K, Iijima T, Miyazaki H, Yasuhara S. The effects of design factors of the combustion chamber on heat balance in a gasoline engine. SAE technical paper 2005-01-2021; 2005, http://dx.doi.org/104271/2005-01-2021.
[101] Esfahanian V, Javaheri A, Ghaffarpour M. Thermal analysis of an SI engine piston using different combustion boundary condition treatments. Applied Thermal Engineering 2006;26:277–87.
[102] Mukai K, Miyazaki H. The influence of the combustion chamber head material of a gasoline engine on exhaust HC. SAE technical paper 2000-01-3072; 2000, http://dx.doi.org/104271/2000-01-3072.
[103] Colaço MJ, Teixeira CV, Dutra LM. Thermal analysis of a diesel engine operating with diesel–biodiesel blends. Fuel 2010;89:3742–52.
[104] Jafari A, Hannani SK. Effect of fuel and engine operational characteristics on the heat loss from combustion chamber surfaces of SI engines. International Communications in Heat and Mass Transfer 2006;33:122–34.
[105] Primus R, Flynn P. The assessment of losses in diesel engines using second law analysis. Computer-Aided Engineering of Energy Systems 1986;3:61–8.
[106] Smith L, Preston W, Dowd G, Taylor O, Wilkinson K. Application of a first law heat balance method to a turbocharged automotive diesel engine. SAE technical paper 2009-01-2744; 2009.
[107] Xin Q, Zheng J. Theoretical analysis of internal combustion engine miscellaneous heat losses. SAE technical paper 2009-01-2881; 2009.
[108] Ottikkutti P. Multizone modeling of a fumigated diesel engine. PhD thesis. Ames, IA: Iowa State University of Science and Technology; 1989.
[109] Li Q. Development of a quasi-dimensional diesel engine simulation for energy and availability analysis. PhD thesis. Urbana-Champaign: University of Illinois; 1992.
[110] Gupta A, Mehta P, Gupta C. Model for predicting air–fuel mixing and combustion for direct injection diesel engine. SAE technical paper 860331; 1986.
[111] McCarthy P, Rasul M, Moazzem S. Analysis and comparison of performance and emissions of an internal combustion engine fuelled with petroleum diesel and different bio-diesels. Fuel 2011;90:2147–57.
[112] Uzun A, Çevik Is, Akçil M. Effects of thermal barrier coating on a turbocharged diesel engine performance. Surface and Coatings Technology 1999;116: 505–507.
[113] Parlak A, Yasar H, Soyhan H, Deniz C. Optimization of an irreversible Diesel cycle: experimental results of a ceramic coated indirect-injection supercharged Diesel engine. Energy & Fuels 2008;22:1930–5.
[114] Rakopoulos C, Giakoumis E. Development of cumulative and availability rate balances in a multi-cylinder turbocharged indirect injection diesel engine. Energy Conversion and Management 1997;38:347–69.
[115] Rakopoulos C, Giakoumis E. Comparative first-and second-law parametric study of transient diesel engine operation. Energy 2006;31:1927–42.